IJCRT.ORG ISSN : 2320-2882

INTERNATIONAL JOURNAL OF CREATIVE RESEARCH THOUGHTS (IJCRT)

An International Open Access, Peer-reviewed, Refereed Journal

WIRELESS POWER TRANSMISSION FOR ELECTRIC VEHICLE

[1]Dr.K.Shivarama krishna, [2]D.Laxman Kumar, [3]M.Harsha Vardhan,[4]P.N.Aparna,[5]N.Navya

[1]Associate Professor of Department of Electrical and Electronics Engineering, [2,3,4,5]Student

[1]J.B.Institute of Engineering and Technology,

[1](Affilicated to Jawaharlal Nehru Technological University, Hyderabad, Telangana) Moinabad , Hyderabad , India

Abstract: Recently available high-frequency power converter topologies for inductive power transfer (IPT) system utilize either zero voltage switching (ZVS) or zero current switching (ZCS) based power electronic converters while maintaining a near sinusoidal current for limited power transfer range. However, achieving ZVS or ZCS for all power switches simultaneously is still a challenging task in IPT systems. In this article, an improved zero-voltage zero-current switching (ZVZCS) IPT topology and its switching pattern are proposed. ZVS is achieved by optimizing the classical series compensation and additionally, an auxiliary network is employed to achieve ZCS. Finally, the practical viability of the proposed topology is validated by the results obtained using a laboratory prototype rated for 1.1 kW, 85 kHz. An efficiency of 91.26% is achieved with ZVZCS for a full dynamic power transfer range of 20 W–1.1.

***KEYWORDS*- Inductive power transfer, Zero voltage switching, Zero current switching, Electric vehicle.**

I. INTRODUCTION

Automation has created a bigger hype in the electronics. The major reason for this type is automation provides greater advantages like accuracy, energy conversation, reliability and more over the automated systems do not require any human attention. Any one of the requirements stated above demands for the design of an automated device. Wireless energy transfer or wireless power is the transmission of electrical energy from a power source to an electrical load without a conductive physical connection. Wireless transmission is useful in cases where interconnecting wires are inconvenient, hazardous, or impossible. The problem of wireless power transmission differs from that of wireless telecommunications, such as radio. In the latter, the proportion of energy received becomes critical only if it is too low for the signal to be distinguished from the background noise. With wireless power, efficiency is the more significant parameter.

A large part of the energy sent out by the generating plant must arrive at the receiver or receivers to make the system economical. The most common form of wireless power transmission is carried out using direct induction followed by resonant magnetic induction.

Automation has created a bigger hype in the electronics. The major reason for this type is automation provides greater advantages like accuracy, energy conversation, reliability and more over the automated s̄ystems do not require any human attention. Any one of the requirements stated above demands for the design of an automated device.

II. OPERATING PRINCIPLE

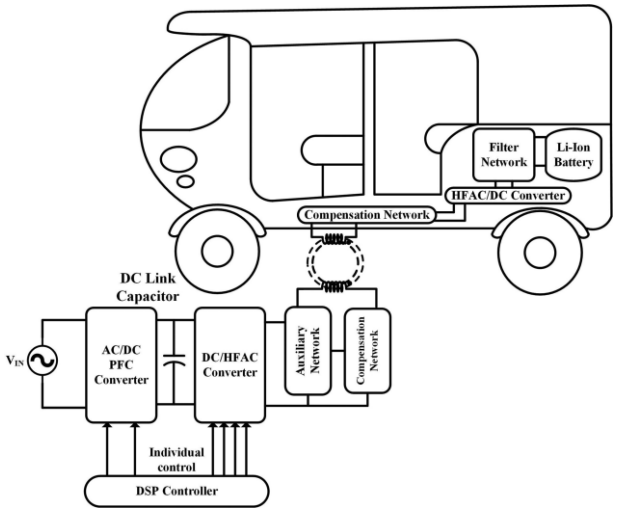

Fig. 1. General configuration of wireless battery charger topology.

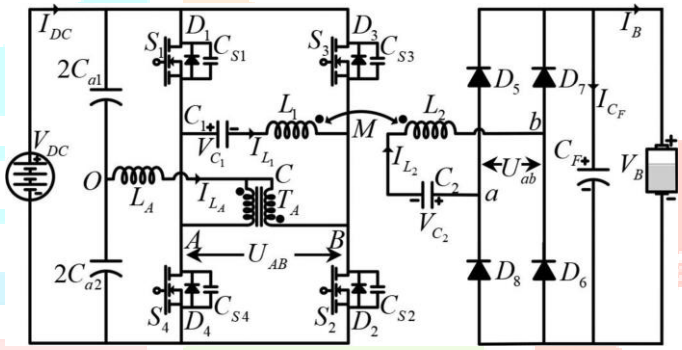

Fig. 2. Proposed network configuration of EV battery charger.

Active switches S_1 - S_2 at primary side and diodes D_5 - D_8 at secondary side forms a H-bridge(conventional).Moreover,C_{a1} and C_{a2} act as potential divider at the input with ancillary L_4 and T_4 to maintain the soft-switching feature of the circuit with BC .The primary and secondary side of the circuit is coupled with L_1 and L_2 with C_1 and C_2 respectively. . The operation of the converter is controlled by using MPWM .

The following assumptions are considered to understand the operating principle of the proposed converter.

All active and passive devices consisting of transformer, dc source, switches, diodes, and capacitors are ideal including internal switch diode and capacitance.

Electrical series resistance of inductor and interwinding capacitance of transformer are neglected.

Voltage divider capacitors ($Ca = Ca_1 = Ca_2$) and C_F are large enough to maintain constant voltage at input and output terminals of the converter .The effects of the magnetizing inductance of TA are neglected.

III. LABORATORY PROTOTYPE

To validate the circuit analysis and simulation results, a laboratory prototype of 1.1 kW at 85 kHz is developed and tested for BC characteristics. The developed prototype primarily composed of five major parts: dc power supply, proposed dc–dc converter, IPT transmitter and receiver coil set, bridge rectifier, resistive, and battery load. A low voltage isolated dc power supply based on bridge rectifier, and linear voltage regulator is developed to active pulse triggering circuit to the dc–dc converter. Open-loop control is used for testing at different charging states of the battery.

TABLE -I

SPECIFICATION OF HARDWARE COMPONENTS

Specifications	Part No.
Power MOSFET	IRFP460
Ultra fast rectifier diode	MUR3060
Gate Driver IC	TC4420, TC4429
Opto-isolator IC	6N137
Line driver IC	74LS04, 74LS07
Digital isolator	ISO7762
Load Resistance	0-25 Ω, 10A wire wound
Voltage regulator IC	LM7815, LM7805
Switch charge control diode	UF4007
DSP Controller	LUNCHXL F28379D
Lithium-Ion	120V, 1.14kVA

In the proposed converter, a split electrolytic capacitor is used to maintain a constant voltage at the input terminal of H-bridge. The driver circuit is placed very near to the switch by utilizing surface mount device technology to reduce any line inductance and circuit positioning effects. The transmitter coil is directly soldered to the converter board with series capacitors to reduce any contact resistances.

The transmitter and receiver coils are placed one meter far from power converter printed circuit board (PCB) to reduce flux linkage and effects on power transmission. The receiver coil is connected in series with a compensation capacitor followed by a diode bridge rectifier and filter capacitor. This dc power is used to test the loading at various battery voltages and load resistors to check performance at dynamic conditions. The presented results are also following a moderate loading of the battery proposed converter operational performance.

IV. WORKING PROCEDURE

Our experiment had six basic parts: the pulse generator, sending coil, receiving coil, rectifier, regulator, and load. The copper coil, illustrated by object A, is a single loop of insulated copper wire. The sending coil and receiving coil are illustrated by objects B and C respectively. These coils of copper tubing are made to be exactly the same so they resonate at the same frequency. The pick-up is object D and is connected in series to a load.

The resonant frequency of our coils, at which we get the most power, varies with the distance between the coils. Due to this we chose to use a frequency generator so that we could adjust the frequency as needed. Several oscillators were built to generate certain frequencies, but due to the varying nature of our resonant frequency, the frequency generator like PIC 16F72 as pulse generator was used. A frequency generator PIC16F72 microcontroller outputs a signal of the same frequency as the resonant frequency of our copper coils, because we can output maximum power at this frequency.

The signal generated is put into our driving loop of 10 gauge wire. The loop is just smaller than our primary coil (approximately 55.5 cm in diameter). The AC current in the driving loop causes the loop of wire to behave like a dipole. The driving loop is positioned parallel to the primary coil, as close as possible. The flux generated by the driving loop through the primary coil causes the coil to resonate. It is important to realize that the driving loop does not make the secondary loop resonate directly. The evanescent waves emitted by the primary coil causes the secondary coil to resonate, because the coils are of the same shape, size, and mass (or close to identical). Both the primary coil and the secondary coil are made of copper tubing that is 1/4 inch inner diameter (3/8 inch outer diameter).

The coils use 60 feet of tubing each, and have about 10 turns (57.5 cm in diameter). At this point the two coils are parallel to each other and resonating, using only enough power to make the driving loop “drive” the first coil. The distance between the primary and secondary coils determines the magnitude of power that is transmitted.

The power exponentially decays as the coils are moved further apart. When the secondary coil vibrates at its resonant frequency, a stronger magnetic field is generated. The receiving loop of 10 gauge wire is situated parallel to the secondary coil, as close as possible. The magnetic flux from the secondary coil induces a current in the receiving loop, which drives a resistive load.

V. RESULTS AND DISCUSSION

The working principle of the proposed converter topology is validated by performing modeling, simulation, and hardware testing. The circuit parameters in simulation and hardware are tuned to an operating point to understand the behavior of the converter.

A. Simulation Results

The simulation of a proposed topology has been done in MATLAB/Simulink by using principal components, as shown in Fig. 2 and Table I. The ideal dc source is placed in series with resistor (nΩ) and inductor (nH). MOSFET switches from SimPowerSystem Library with 0 Ω resistance and 870 pF capacitance as snubber have been used to simulate H-bridge part of dc–dc converter. The auxiliary transformer is contracted by linear transformer and transmitter, receiver coils from mutual inductance.

Fig. 4 shows the ZVS turn-ON of switches S1 to S4, as the voltage across the switch reaches to zero, the gate pulse is given to that particular switch to turn it ON. In Fig. 5(a) and (b), the ZCS turn-ON for switches S2 and S4 is indicated. The current from the switch becomes zero before the gate pulse finishes. Therefore it is said that the proposed wireless converter maintains ZCZVS. The compensation capacitor voltage peak value is selected by observing the performance of VC1 , as shown in Fig. 6. In Fig. 7, the input side characteristic of the primary network has been shown. These results show the small value of input dc-link capacitors does not affect the performance of the converter.

The performance of the converter for BC is shown in Fig. 8(a)–(d). It is seen from Fig. 8(a) and (b) that the disturbance is very less, whereas the conventional charger having disturbance in BC voltage and current, which reduces the life of the battery and degrades the charger efficiency, whereas the nature of battery voltage and current shown in Fig. 8(c) and (d) is without using the auxiliary circuit. The circuit performance provides 93.5% efficiency with parameters shown in Table I. The output efficiency for fixed parameters is controlled by updating the switching frequency and output power is controlled by changing input voltage. A lookup table has been used to find control parameters. The simulation parameters are obtained from component data-sheet and careful study of the developed prototype in the laboratory.

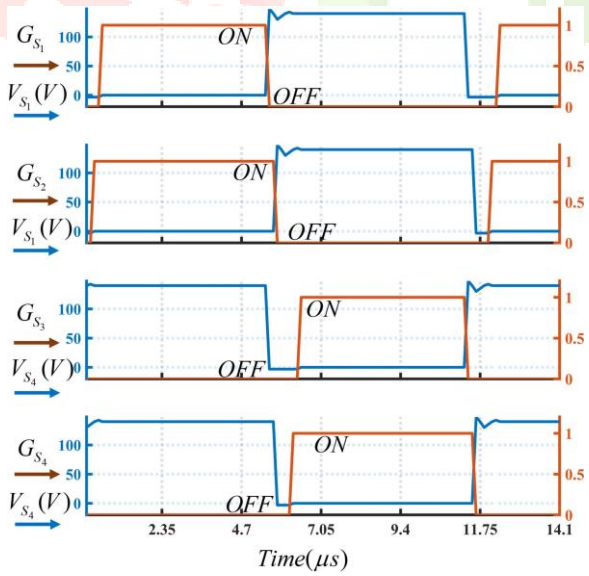

Fig. 4. ZVS turn-ON for S1 − S4.

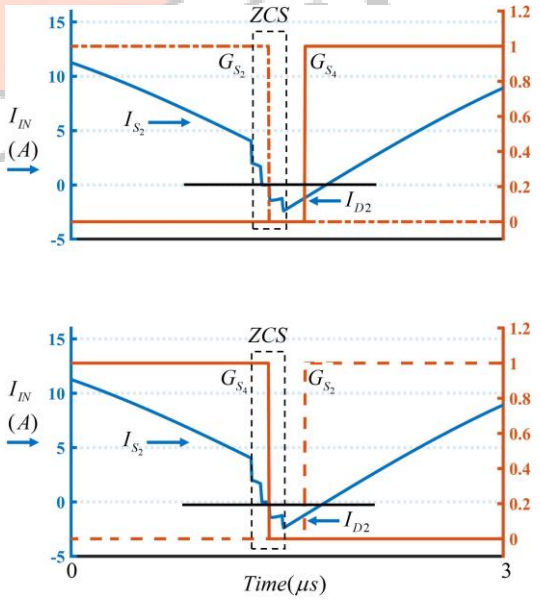

Fig. 5. ZCS turn-OFF for (a) S2 and (b) S4.

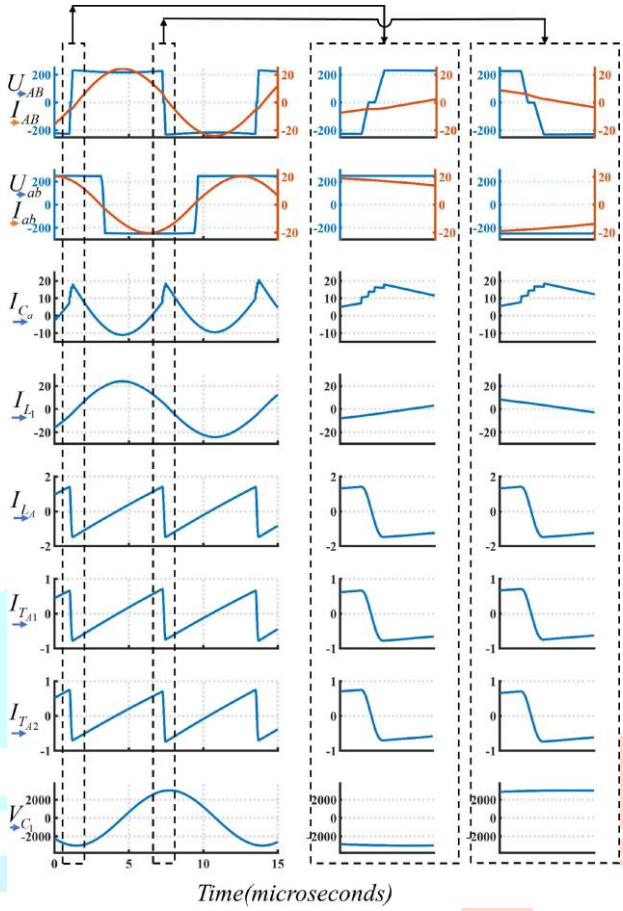

Fig. 6. Converter characteristics waveform in various operating modes.

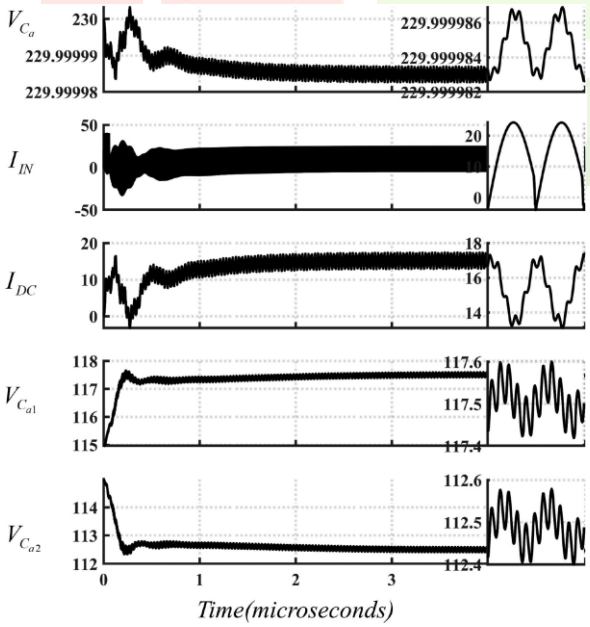

Fig. 7. Input side characteristic of primary network.

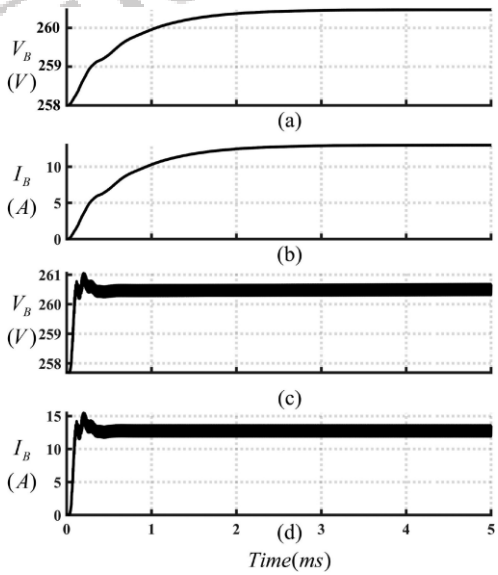

Fig. 8. output side characteristic of primary network.

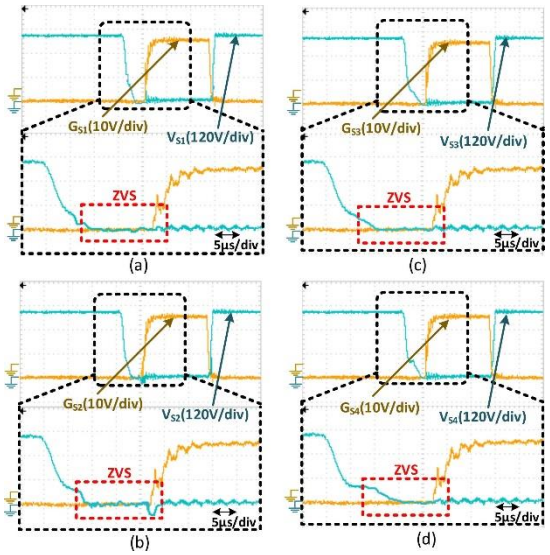

Fig. 9. Experimental results of ZVS turn-ON for (a)–(d) $S_1 - S_4$.

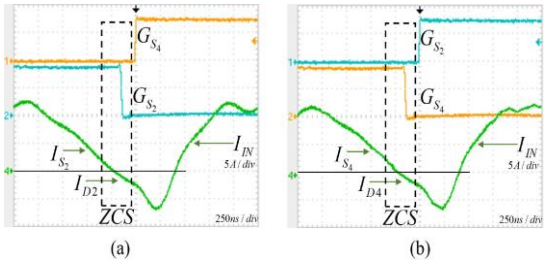

Fig. 10. Experimental results of ZCS turn-OFF for (a) S_2 and (b) S_4.

B. HARDWARE RESULT

The developed laboratory prototype is tested forboth high-power and low-power BC. The obtained results showthe ZCZVS soft switching is obtained for a wide operating range.In Fig. 9(a)–(d), the ZVS turn-ON of switches S_1 S_4 is shown,when the voltage across the switch is zero then the switch willtriggered. The ZCS turn-OFF of two low-side switches S_2 and S_4 is shown in Fig. 10(a) and (b).

The voltage appear across primary and secondary of the con-verter at points *A*, *B* and *a*, *b* is shown in Fig. 11(a), Fig. 11(b) and (c) shows the voltage across battery and current flowing through L_1. The input current, dc current, and current across capacitor potential divider are shown in Fig. 12(a)–(d), respectively. Theseresults satisfy the theoretical operation as well as simulation ofthe proposed converter.

Fig. 13(a) shows the BC characteristics for 120-V Li-ion bat-tery with a proposed auxiliary circuit. The current in the circuitis 4.35 A, which delivers 522 W at 91.26% efficiency. Fig. 13(b)shows the BC current and voltage in heavy loading conditions. The delivered power is measured at 1028 W at 91.02% efficiency.

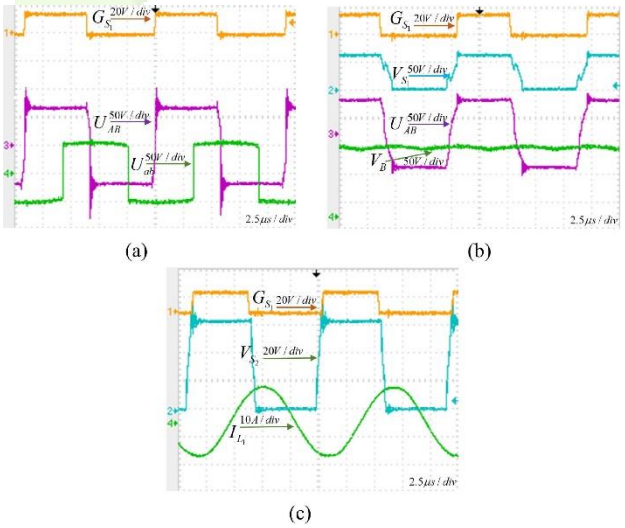

Fig. 11. Laboratory prototype results for (a) voltage across points *A*, *B* and *a*,*b*, (b) battery voltage w.r.t. voltage across points *A* and *B*, and (c) current passing through transmitter coil.

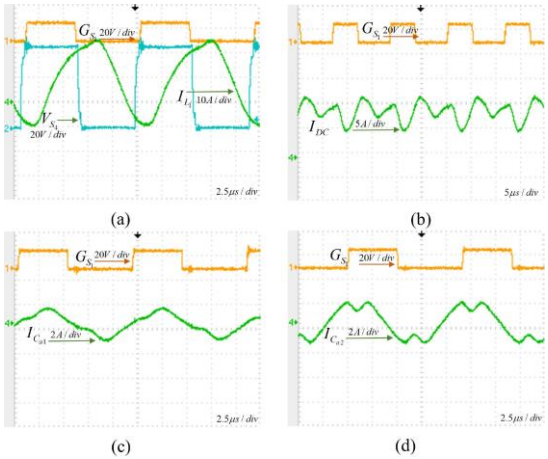

Fig. 12. (a) Input current passing through S_1. (b) DC current coming from supply. (c), (d) Current passing through capacitor potential divider.

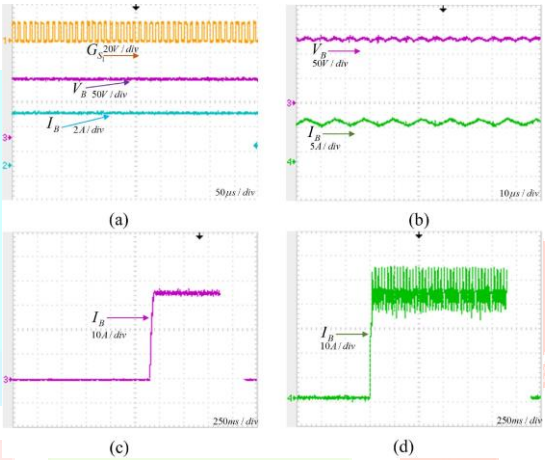

Fig. 13. (a) Battery voltage and current, (b) magnified voltage and current ofbattery load, transient state of battery current (c) with the proposed auxiliary circuit, and (d) without auxiliary circuit.

The start-up BC characteristics for the proposed auxiliary or the transient current of BC are shown in Fig. 13(c) and without auxiliary network the transient current is shown in Fig. 13(d). It is observed the startup time is less for the proposed circuit but the ripple is high. On the other hand, the spikes are more when no auxiliary circuit has been incorporated.

VI. CONCLUSION

Integrating features of all the hardware components used have been developed in it. Presence of every module has been reasoned out and placed carefully, thus contributing to the best working of the unit. Secondly, using highly advanced IC's with the help of growing technology, the project has been successfully implemented. Thus the project has been successfully designed and tested.

The offered solution produced less ripple in input/ outputvoltage and current while utilizing a low value of dc link, and filter capacitance values, respectively. An acceptable efficiencyof 91.26% has been achieved for both battery and resistive loads.

VII. ACKNOWLEDGMENT

At outset we express our gratitude to almighty lord for showering his grace and blessings upon us to complete this Main Project. Although our name appears on the cover of this book, many people had contributed in some form or the other to this project development. We could not have done this Project without the assistance or support of each of the following.

First of all, we are highly indebted to Dr. P. C. KRISHNAMACHARY, Principal for giving us the permission to carry out this Main Project.

We would like to thank Dr. P. DURAIPANDY, Associate Professor & Head of the Department of Electrical & Electronics Engineering**,** for being moral support throughout the period of the study in the Department.

We are grateful to Dr. K. SHIVARAMA KRISHNA, Associate Professor of the Department of Electrical & Electronics Engineering, for his valuable suggestions and guidance given by him during the execution of this Project work.

We would like to thank Teaching and Non-Teaching Staff of Department of Electrical & Electronics Engineering for sharing their knowledge with us.

VIII. REFERENCES

[1] M. Granovskii , I. Dincer, and M. A. Rosen, "Economic and environmental comparison of conventional, hybrid,electric and hydrogen fuel cell vehicles," J. Power Sources, vol. 159, no. 2, pp. 1186–1193, 2006.

[2] S. B. Peterson, J. Whitacre, and J. Apt, "The economics of using plug-inhybrid electric vehicle battery packs for grid storage," J. Power Sources ,vol. 195, no. 8, pp. 2377–2384, 2010.

[3] Y. Zhou, M. Wang, H. Hao, L. Johnson, and H. Wang, "Plug-in electricvehicle market penetration and incentives: A global review," Mitigation Adaptation Strategies Global Change, vol. 20, no. 5, pp. 777–795, 2015.

[4] B. Nykvist and M. Nilsson, "Rapidly falling costs of battery packs forelectric vehicles," Nature Climate Change, vol. 5, no. 4, pp. 329–332,2015.

[5] W. Zhang and C. C. Mi, "Compensation topologies of high-power wireless power transfer systems," IEEE Trans. Veh. Technol., vol. 65, no. 6, pp. 4768–4778, Jun. 2016.

[6] K. Mude and K. Aditya, "Comprehensive review and analysis oftwo-element resonant compensation topologies for wireless inductive power transfer systems," Chin. J. Elect. Eng., vol. 5, no. 2, pp. 14–31,2019.

[7] Y. Jiang, L. Wang, Y. Wang, J. Liu, X. Li, and G. Ning, "Analysis, design,and implementation of accurate ZVS angle control for EV battery charging in wireless high-power transfer," *IEEE Trans. Ind. Electron.*, vol. 66, no. 5,pp. 4075–4085, May 2019.

[8] Y. Jiang, L. Wang, Y. Wang, J. Liu, M. Wu, and G. Ning, "Analysis, design,and implementation of WPT system for EV's battery charging based on optimal operation frequency range," *IEEE Trans. Power Electron.*, vol. 34, no. 7, pp. 6890–6905, Jul. 2019.

[9] D. H. Tran, V. B. Vu, and W. Choi, "Design of a high-efficiency wirelesspower transfer system with intermediate coils for the on-board chargers of electric vehicles," *IEEE Trans. Power Electron.*, vol. 33, no. 1, pp. 175–187, Jan. 2018.

[10] S. Moon and G.-W. Moon, "Wireless power transfer system with anasymmetric four-coil resonator for electric vehicle battery chargers," *IEEETrans. Power Electron.*, vol. 31, no. 10, pp. 6844–6854, Oct. 2016.

[11] O. C. Onar, M. Chinthavali, S. L. Campbell, L. E. Seiber, and C. P. White,"Vehicular integration of wireless power transfer systems and hardware interoperability case studies," *IEEE Trans. Ind. Appl.*, vol. 55, no. 5, pp. 5223–5234, Sep./Oct. 2019.

[12] S. Li, W. Li, J. Deng, T. D. Nguyen, and C. C. Mi, "A double-sided LCC compensation network and its tuning method for wireless power transfer," *IEEE Trans. Veh. Technol.*, vol. 64, no. 6, pp. 2261–2273, Jun. 2015.

[13] C. Liu, S. Ge, Y. Guo, H. Li, and G. Cai, "Double-LCL resonant compensation network for electric vehicles wireless power transfer: Experimental study and analysis," *IET Power Electron.*, vol. 9, no. 11, pp. 2262–2270, 2016.

[14] C. Xiao, D. Cheng, and K. Wei, "An LCC-C compensated wireless charging system for implantable cardiac pacemakers: Theory, experiment, and safety evaluation," *IEEE Trans. Power Electron.*, vol. 33, no. 6, pp. 4894–4905, Jun. 2018.

[15] Y. Chen, H. Zhang, S.-J. Park, and D.-H. Kim, "A switching hybrid LCC-S compensation topology for constant current/voltage EV wireless charging," *IEEE Access*, vol. 7, pp. 133924–133935, 2019.

[16] Y. Zhang, Z. Yan, T. Kan, Y. Liu, and C. C. Mi, "Modelling and analysis of the distortion of strongly-coupled wireless power transfer systems with SS and LCC–LCC compensations," *IET Power Electron.*, vol. 12, no. 6, pp. 1321–1328, 2019.

[17] W. Li, H. Zhao, J. Deng, S. Li, and C. C. Mi, "Comparison study on SSand double-sided LCC compensation topologies for EV/PHEV wireless chargers," *IEEE Trans. Veh. Technol.*, vol. 65, no. 6, pp. 4429–4439, Jun. 2016

[18] Rajasekhar Gorthi, K.Giribabu, Dr.Shivaprasad: Simulink model for Cost-effective analysis of Hybrid system: International journal of odern Engineering Research (Volume:4,Issue:2, Feb 2014)

[19] Dr .Rajesh Thipparaju , Suddala Janardhan, Rajasekhar Gorthi: PV array based BLDC motor driven water pump using solar Technology: The International Journal of analytical and experimental model analysis(Volume:12,Issue:7, July 2020)